ADVANCES IN ATMOSPHERIC SCIENCES, VOL. 29, NO. 6, 2012, 1129–1141

Relationship between ENSO and Winter Rainfall over Southeast China and Its Decadal Variability

LI Chun*[1] (李 春) and MA Hao[2] (马 浩)

[1] *Physical Oceanography Laboratory and Key Laboratory of Ocean-Atmosphere Interaction and Climate in Universities of Shandong, Ocean University of China, Qingdao* 266100

[2] *Zhejiang Province Climate Center, Hangzhou* 310017

(Received 30 November 2011; revised 27 January 2012)

ABSTRACT

In this study, the relationship between El Niño-Southern Oscillation (ENSO) and winter rainfall over Southeast China (SC) is demonstrated based on instrumental and reanalysis data. The results show that ENSO and SC winter rainfall (ENSO-SC rainfall) are highly correlated and intimately coupled through an anomalous high pressure over the northwestern Pacific. In mature phase, El Niño (La Niña) events can cause more (less) rainfall over SC in winter. Due to the persistence and spring barrier of ENSO, SC winter rainfall has potential predictability of about half a year ahead with ENSO as a predictor.

Besides, the ENSO-SC rainfall relationship exhibits decadal variability, closer before the early 1970s (0.47) and after the early 1990s (0.76), but weaker (0.12) between these times. In different periods, atmospheric teleconnection patterns have large differences and the predictability of SC winter rainfall also changes dramatically. For the most recent 20 years, the ENSO-SC rainfall relationship is closest and the prediction of SC winter rainfall anomalies based on ENSO is most creditable. In addition, the causes and mechanisms of the decadal modulation of the relationship between ENSO and SC winter rainfall need to be further studied.

Key words: ENSO, winter rainfall, decadal variability, atmospheric teleconnection, predictability

Citation: Li, C., and H. Ma, 2012: Relationship between ENSO and winter rainfall over Southeast China and its decadal variability. *Adv. Atmos. Sci.*, **29**(6), 1129–1141, doi: 10.1007/s00376-012-1248-z.

1. Introduction

El Niño-Southern Oscillation (ENSO), the strongest interannual air–sea coupled mode, exerts significant impacts on global climate, including the East Asian monsoon (Alexander et al., 2002). Previous monsoon research has mainly focused on summer rainfall because of its enormous social and economic benefits (e.g. Fu and Teng, 1988; Huang and Wu, 1989; Ju and Slingo, 1995; Zhang et al., 1996; Webster et al., 1998; Tao and Zhang, 1998). Studies have suggested that ENSO can affect East Asian climate through Rossby waves mediated by the Pacific–East Asian (EAP) teleconnection in the lower troposphere (Wang et al., 2000). Based on singular value decomposition (SVD) analysis, Lau and Weng (2001) found that summer rainfall variability over China is associated with several different global sea surface temperature (SST) modes, and the 1997/98 rainfall anomalies over China can be explained by the mode representing the growing phase of El Niño and the mode representing the transition from El Niño to La Niña phases, respectively. In recent years, Yang et al. (2007) and Xie et al. (2009) demonstrated that basin-wide SST anomalies in the Indian Ocean can influence summer rainfall over China via the "capacitor effect". The tropical Indian Ocean SST increases in response to the atmospheric teleconnection forced by an El Niño event, which is similar to a battery charging a capacitor. The tropical Indian Ocean warming persists through the following summer and exerts its climatic influence on East Asia via the Pacific–Japan (P–J) teleconnection after the El Niño event, like a discharging capacitor. The capacitor effect appears to be stronger after the

*Corresponding author: LI Chun, lichun7603@ouc.edu.cn

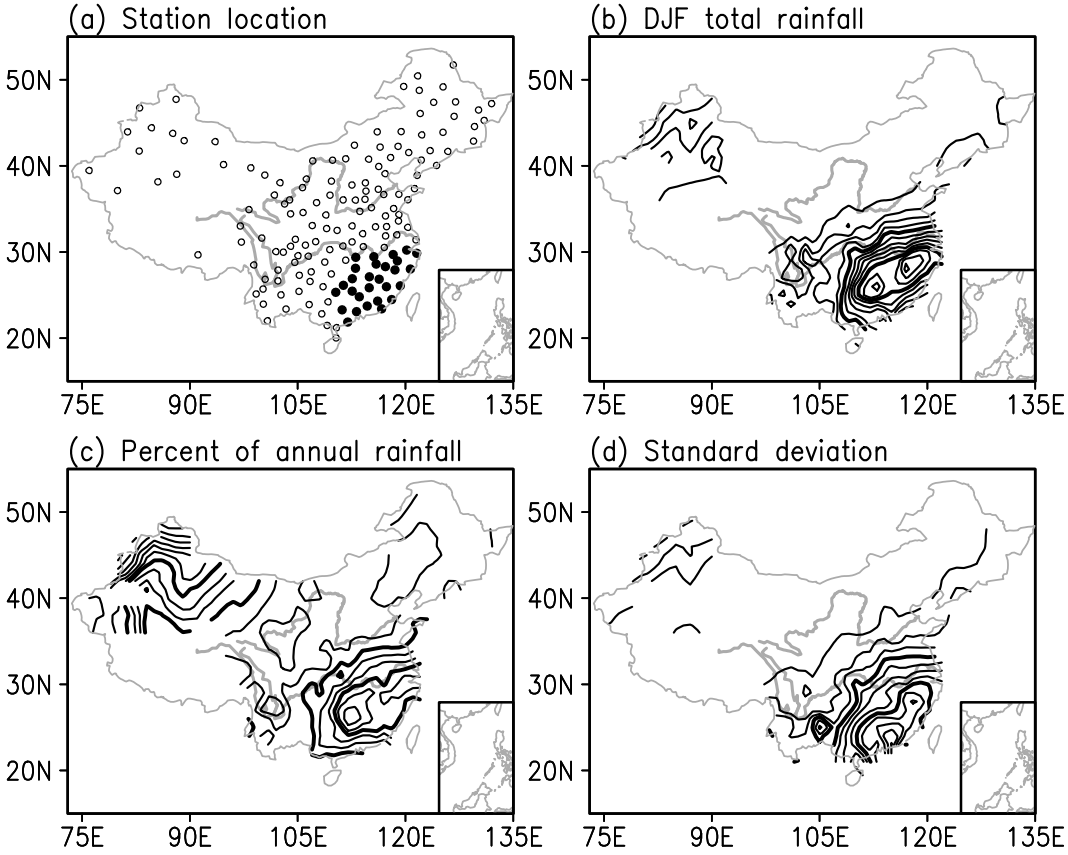

Fig. 1. (a) Locations of the 160 stations used for calculating precipitation in China (solid circles denote stations in SC). (b) Winter total rainfall (contour intervals [CIs] at 20, 100 and 200 mm contours are shown as thickened lines). (c) Percentage of annual total rainfall in winter (CIs at 2%, 6% and 12% contours are shown as thickened lines). (d) Standard deviation of winter rainfall (CIs at 10, 40 and 80 mm contours are shown as thickened lines).

1976/77 Pacific decadal climate shift (Xie et al., 2010).

Impacts of ENSO on winter rainfall over China have also been explored. However, compared to summer rainfall, the number of studies is far less, which may be due to much less rainfall in the cold season. In winter, total rainfall is generally less than 50 mm (Fig. 1b), accounting for less than 5% of annual total rainfall (Fig. 1c). Nevertheless, winter rainfall can total more than 100 mm, and the maximum value can rise up to 260 mm in Southeast China (SC) (Fig. 1b), which accounts for 10%–16% of annual total rainfall (Fig. 1c). Meanwhile, the rainfall amplitude also displays large interannual variability and its standard deviation can reach 50–130 mm, about half of SC winter total rainfall (Fig. 1d). Therefore, such rich winter rainfall in SC should not be neglected, and studies on the variability and predictability of SC winter rainfall have distinct climatic, social and economic benefits.

Tao and Zhang (1998) discovered that winter rainfall over SC is more (less) during El Niño (La Niña) years by composite analysis. Wu et al. (2003) studied the evolution of ENSO-related rainfall anomalies in East Asia and pointed out the positive correlation of ENSO and SC winter rainfall by conducting correlation and SVD analyses between seasonal-mean rainfall over China and SST fixed in winter. During El Niño years, more rainfall over SC in winter was observed associated with anomalous low-level southwesterly winds to the northwest flank of an anomalous anticyclone over the northwestern Pacific (Wu et al., 2003; Zhou et al., 2010; Zhou and Wu, 2010). Such anomalous anticyclones, which are triggered by El Niño events, helping us to understand the influences that El Niño events have on summer rainfall anomalies over China (Wang et al., 2000), can also be used to explain winter rainfall anomalies over SC during El Niño years.

Previous studies on positive correlations between ENSO and SC winter rainfall anomalies are useful for predicting future SC winter rainfall anomalies. In fact, SC winter rainfall anomalies can be predicted very well based on ENSO in some years, but in other years, ENSO is not so effective for projecting changes in

SC winter rainfall anomalies. For example, SC winter rainfall was less in the 1976/77 and 1986/87 El Niño years. We found that the interannual relationship between ENSO and SC winter rainfall exhibits interdecadal oscillation, and atmospheric teleconnection displays large differences during different periods. Thus, it is more important to investigate the low-frequency variability of the interannual relationship between ENSO and SC winter rainfall.

This paper is organized as follows. A brief description of the data and methods are given in the next section. In the third section, the dominant ENSO-SC rainfall mode and the possible formation mechanism are discussed. The fourth section demonstrates the potential predictability of SC winter rainfall based on ENSO. Interdecadal variability of the ENSO-SC rainfall relationship is given in the fifth section. A short summary and further discussion are provided in the last section.

2. Data and methods

To investigate the relationship between ENSO and SC winter rainfall, monthly gauge-observed rainfall data over China and global SST reanalysis data were used. Monthly rainfall based on observations from 160 stations was adopted from the data center of the Chinese Meteorological Administration (CMA) (Fig. 1a). This rainfall dataset, from January 1951 to February 2011, has been used extensively in other studies (e.g. Lau and Weng, 2001; Li et al., 2011; Li and Ma, 2011). The monthly SST data were taken from the National Ocean and Atmospheric Administration (NOAA) extended reconstructed SST (ERSST) dataset, provided by the NOAA-Cooperative Institute for Research in Environmental Sciences (NOAA-CIRES) Climate Diagnostics Center (Smith and Reynolds, 2003). The NOAA ERSST (version 3) data have a resolution of 2°×2° and cover the period 1854–2011 (http://www.esrl.noaa.gov/psd/data/gridded/data.noaa.ersst.html). In addition, monthly Kaplan SST and Hadley Center Sea Ice and SST (HadISST) data were also used to examine the reliability of the relationship between ENSO and SC winter rainfall. Kaplan Extended SST (version 2) data, taken from the NOAA-Earth System Research Laboratory (NOAA-ESRL), have a resolution of 5°×5° and cover the period 1854–2011 (www.esrl.noaa.gov/psd/data/gridded/data.kaplan_sst.html) (Kaplan et al., 1998), while the HadISST data, taken from datasets of Met Office Hadley Center observations, have a resolution of 1°×1° and cover the period of 1870–2011 (www.metoffice.gov.uk/hadobs/hadisst/data/download.html) (Rayner et al., 2003). In order to study the linkage between ENSO and SC winter rainfall, monthly atmospheric reanalysis data (including geopotential height, horizontal wind and specific humidity), taken from the National Center for Environmental Prediction/National Center for Atmospheric Research (NCEP/NCAR) reanalysis dataset (Kalnay et al., 1996), were also used, and these data have a resolution of 2.5°×2.5° and cover the period 1948–2011. In order to unify the time-span, all data used in this study cover the period January 1951 to February 2011.

Empirical Orthogonal Function (EOF) analysis was used to extract the dominant mode of global SST and rainfall over China in boreal winter. To identify the covariability relationship between rainfall and SST anomalies, SVD analysis was employed following Lau and Weng (2001), with a focus on boreal winter instead of summer. It should be noted that winter and summer are defined here as traditional December–January–February (DJF) and June–July–August (JJA) means, respectively. Both correlation and regression analyses were applied to confirm the linkage between ENSO and SC winter rainfall. To examine the stability of the ENSO-SC rainfall mode, a running correlation with an 11-year moving widow was also used.

3. Dominant ENSO-SC rainfall mode

3.1 *ENSO-SC rainfall mode*

To study the relationship between global SST and rainfall over China in boreal winter, EOF analyses were first performed to extract the leading modes of global SST and rainfall over China in winter, respectively (Fig. 2). The leading EOF mode of SST explains 24.4% of total variance of global winter SST and shows a typical El Niño-like SST pattern with strong warm anomalies in the tropical central-eastern Pacific and cold anomalies in both its flanks (Fig. 2a). In addition, warm anomalies also occupied the entire Indian Ocean basin (IOB), South China Sea (SCS), East China Sea (ESC) and the tropical Atlantic, while high latitude regions in both the northern and southern Atlantic featured weak cold anomalies. The leading EOF mode of rainfall explains 49.3% of total variance of winter rainfall over China and is characterized by significantly more rainfall over southeastern China (Fig. 2b). The principal components (PCs) of global SST and rainfall over China are correlated at 0.47 during the past six decades in winter (Fig. 2c), exceeding the 99% confidence level. The positive correlation between PCs of global SST and rainfall over China indicates that warm (cold) phases of the ENSO cycle correspond to more (less) rainfall in SC.

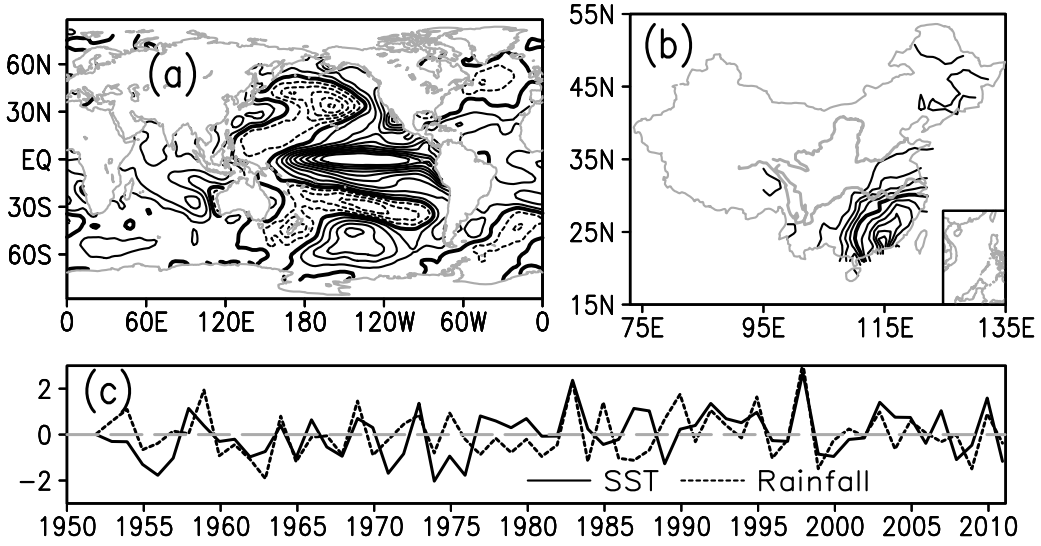

Fig. 2. Leading EOF modes of (a) winter global SST (CIs at 0.1°C and 0°C isotherms are shown as thickened lines); (b) rainfall over China (CIs at 10 and 50 mm contours are shown as thickened lines); and (c) their respective PCs.

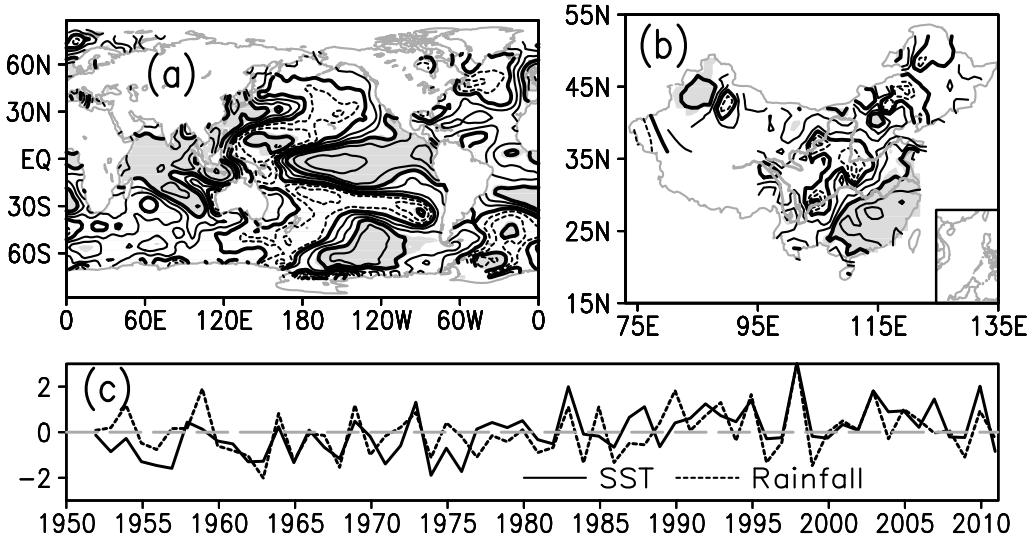

Fig. 3. Spatial heterogeneous pattern of the leading SVD mode of (a) SST; (b) rainfall over China in boreal winter; and (c) their corresponding time series. Contour intervals at 0.1, 0 and ±0.3 contours are shown as thickened lines. Shaded areas exceed the 95% confidence level by the student's *t*-test.

To further confirm the covariability of ENSO and SC winter rainfall, SVD analysis between the winter rainfall over China and simultaneous global SST anomalies was conducted (Fig. 3). The leading SVD mode accounts for 38.9% of the total squared covariance, and explains 14.4% and 15.7% of the variances of SST and rainfall, respectively. The SST pattern also shows a typical El Niño-like pattern, with significant warm anomalies in the tropical central-eastern Pacific, the entire IOB, China marginal seas and the Kuroshio-extension region, while the significant cold anomalies occupy the tropical western Pacific. As for the spatial pattern, SST of the leading SVD mode pattern is highly correlated with that of the leading EOF mode at 0.76 (Fig. 2a vs Fig. 3a). Coupled with the typical El Niño-like SST pattern, the heterogeneous rainfall pattern shows more rainfall localized over the SC region, while a little less rainfall distributed over central

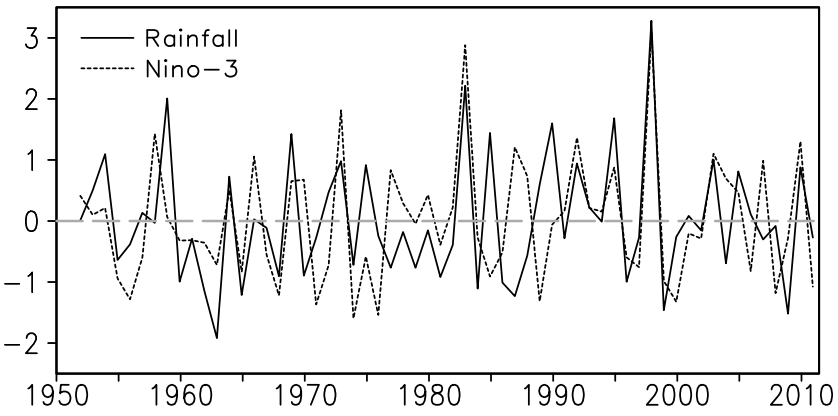

Fig. 4. Normalized SC winter rainfall index (solid line) and Niño-3 index (dashed line).

and northeastern China (Fig. 3b). Also, with respect to the spatial pattern, rainfall over China in boreal winter of the leading SVD mode is highly correlated with that of the leading EOF mode at 0.63 (Fig. 2b vs Fig. 3b). The corresponding time series of the leading SVD mode between global SST and rainfall over China are correlated at 0.63 (Fig. 2c), exceeding the 99% confidence level. Our SVD analysis further indicates that ENSO and SC winter rainfall work as a pair of covariant modes, and we call this the ENSO-SC rainfall mode.

The leading modes of EOF and SVD analyses may be artificial, due to the mathematical influence of the two statistical methods. To remove such an influence, time series of Niño-3 SST and SC winter rainfall indices [averaged from rainfall observations across 28 stations (Fig. 1a with close cycle)] are shown in Fig. 4. Niño-3 and SC winter rainfall indices show the covariant interannual variability and significantly correlate at 0.50 in the past six decades, exceeding the 99% confidence level. This further supports the relationship between ENSO and SC winter rainfall indicated by the EOF and SVD analyses reported above.

However, our results may depend on the SST data itself. Therefore, to check the objectivity of the covariant mode between ENSO and SC winter rainfall, EOF and SVD analyses were repeated based on the Kaplan SST and HadISST data (not shown).The results were generally consistent with each other, and thus the covariant mode of ENSO-SC winter rainfall is a robust mode.

3.2 *Possible mechanism of the ENSO-SC rainfall mode*

So far, it remains unclear as to what the mechanisms conveying the remote influences of the ENSO to the SC region are, and how this affects local precipitation. It is conceivable that mature El Niño can trigger Rossby waves propagating westward (Wang et al., 2000), setting up an anomalous anticyclone by local positive wind-evaporation-SST (WES) feedback (Xie and Philander, 1994) in the northwestern tropical Pacific. During the mature phase of El Niño events, the tropical central-eastern Pacific is covered by warm SST anomalies, which induce cold SST anomalies in the western Pacific. The western North Pacific anticyclone is first originated from anomalous cooling in the western Pacific, and positive ocean–atmosphere coupled thermodynamic feedback works to amplify and propagate the initial anticyclone, finally producing a massive western North Pacific anticyclone. It should be noted that besides local cold SST anomalies, central-eastern Pacific warming also plays an important role in the development and maintenance of Philippine anticyclones. The mechanism was used to understand the influences of ENSO on summer rainfall over China (Wang et al., 2000). However, the mechanism may also be used to explain impacts of mature ENSO on winter rainfall over the SC region (Wu et al., 2003; Zhou and Wu, 2010). To demonstrate this fact, geopotential height, horizontal wind and whole-layer moisture transport are regressed against DJF Niño-3 SST index (Figs. 5, 6), respectively.

The atmospheric circulation shows quasi-barotropic anomalies with an anomalous ridge stretching northwestward in the Northwest Pacific and a strong (weak) anomalous trough over the Aleutian low region (continental China), while the amplitudes are enhanced from low to high levels (Fig. 5). The anomalous ridge weakens the East Asian trough, reduces meridional air mass exchange, and further weakens the East Asian winter monsoon, so causing anomalous warming over China in winter (not shown), which is consistent with previous studies. At the upper level in the troposphere, associated with the anomalies low over continental China and the anomalous ridge in the

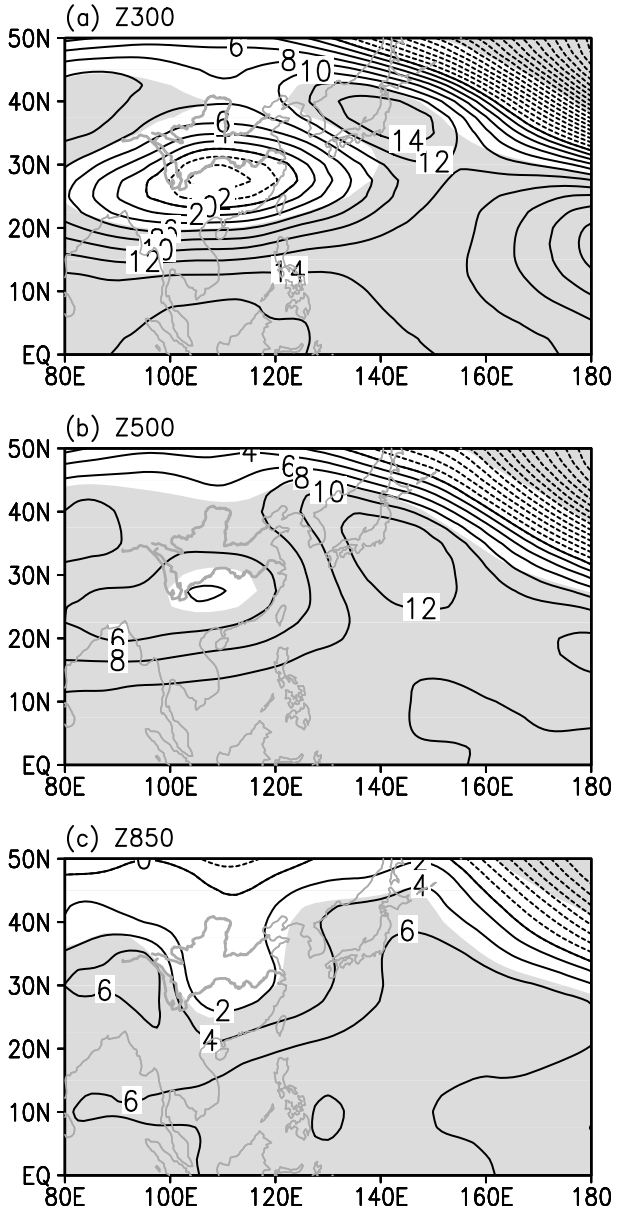

Fig. 5. Regression of DJF geopotential height at (a) 300 hPa; (b) 500 hPa; and (c) 850 hPa (units: gpm) on normalized PC1 of SST. Shaded areas exceed the 95% confidence level.

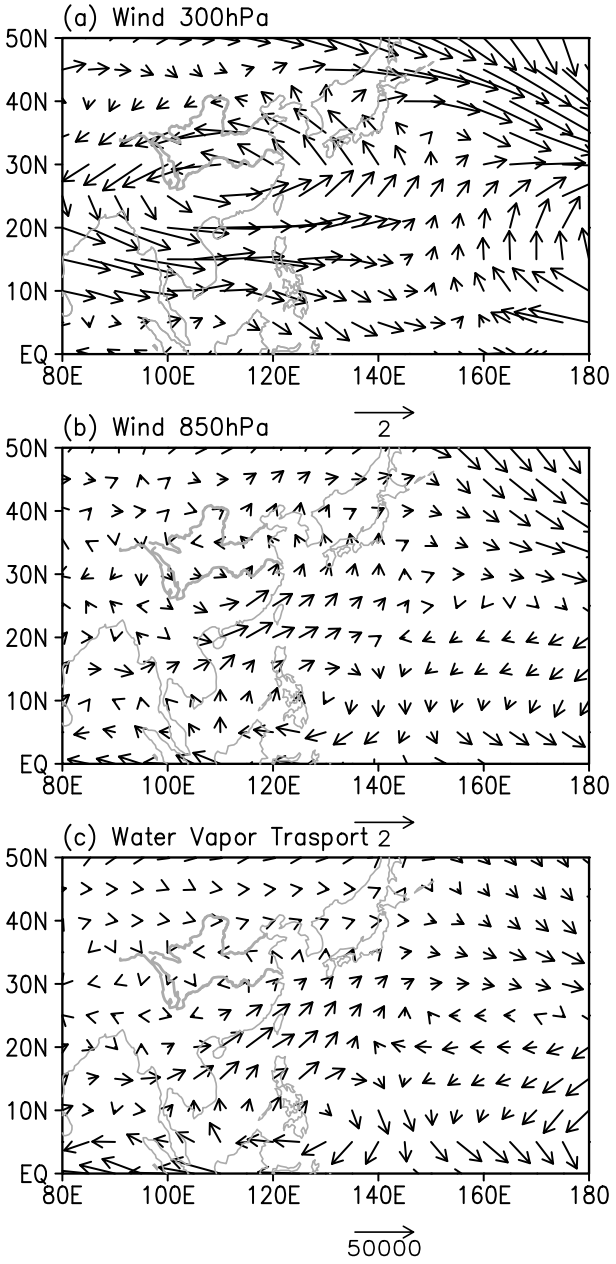

Fig. 6. Regression of DJF horizontal wind at (a) 300 hPa; (b) 850 hPa (units: m s^{-1}); and (c) whole-layer moisture transport (units: g m^{-1} s^{-1}) on normalized PC1 of SST.

mid-latitude northwestern Pacific, there exhibits corresponding cyclonic and anticyclonic wind anomalies, respectively (Figs. 5a and 6a). Similarly, at the lower level, the anomalous weak trough is related to the cyclonic wind anomalies over the SC region and the anomalous high corresponds to anticyclonic wind anomalies (Figs. 5c and 6b) in the Northwest Pacific. The anomalous trough in the SC region and ridge in the Northwest Pacific work jointly to cause the southwesterly wind anomalies in the northwestern flank of the anomalous anticyclone in the Northwest Pacific, and such anomalous southwesterly wind transports moisture and induces moisture to converge toward the SC region (Fig. 6c), which favors more winter rainfall over the SC. Therefore, the anomalous anticyclone plays a vitally important role in linking ENSO with SC winter rainfall anomalies (Wu et al., 2003; Zhou et al., 2010).

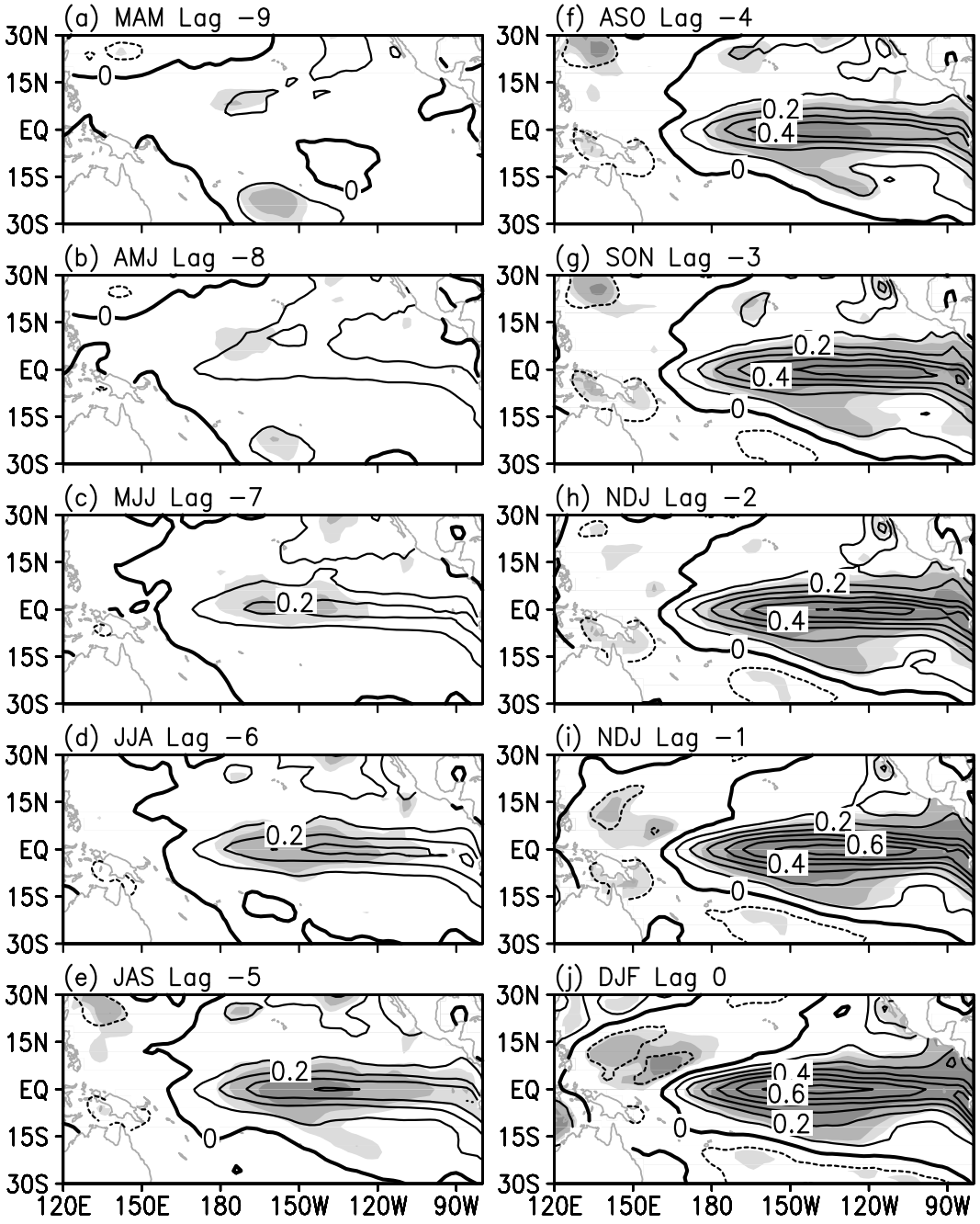

Fig. 7. Lagged regressions between SST and normalized PC1 of winter rainfall over China. Contour intervals at 0.1°C and 0°C lines are thickened. Shaded areas from light to dark denote regions with correlations significant at the 0.05, 0.01 and 0.001 levels, respectively.

4. Potential predictability of SC winter rainfall

Our above-reported analyses indicate that the covariant relationship between ENSO and SC winter rainfall is robust in winter. Given this, it becomes important to ask whether SC winter rainfall can be predicted by ENSO-related SST anomalies in the tropical central-eastern Pacific. If yes, how far ahead can SC winter rainfall be predicted? To assess the potential predictability, lagged regressions of tropical Pacific SST against the SC winter rainfall normalized index were calculated (Fig. 7).

The significant correlation first emerges near the Niño-3.4 region (5°S–5°N, 170°–120°W) in early summer (May–June–July; MJJ) (Fig. 7c), which implies

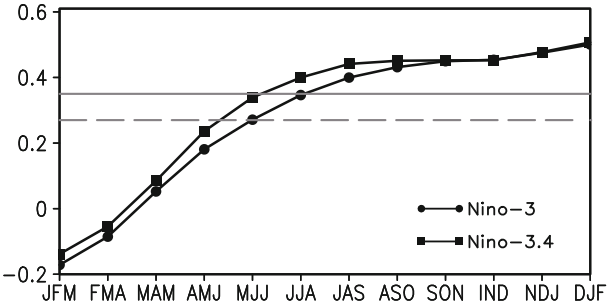

Fig. 8. Lagged correlations of Niño-3 and Niño-3.4 SST indices with the SC winter rainfall index for the past six decades. Dashed and solid gray lines denote correlations significant at the 0.05 and 0.01 levels, respectively.

there is a maximum seven months potential predictability. In fact, the correlation in the Niño-3.4 region only exceeds the 95% confidence level and cannot pass the 99% level in MJJ. Later, the correlation gradually becomes more and more significant and extends eastward from the central to eastern tropical Pacific with the development of the ENSO event. In summer (JJA), the significant correlation extends eastward to 100°W and appears exceeding the 99% confidence level in the Niño-3.4 region (Fig. 7d). In late summer (July–August–September; JAS), the significant correlation further extends to the east coast of the tropical Pacific and exceeds the 99.9% confidence level in the Niño-3.4 region (Fig. 7e). In autumn (September–October–November; SON), the high correlation region spreads to the entire tropical central-eastern Pacific (Fig. 7g), and then maintains to reach the mature phase of ENSO in winter (Figs. 7h–j).

The above-reported correlation analyses suggest that SC winter rainfall may be predicted by ENSO for six–seven months ahead. The lagged correlation of the SC winter rainfall index with the Niño-3 and Niño-3.4 SST indices further confirm the prediction timescale of SC winter rainfall (Fig. 8).

However, it remains elusive as to why the prediction timescale is about six–seven months ahead. In order to address this question, the persistent barrier was examined by calculating the autocorrelations of the Niño-3 SST index (Table 1), following Chen et al. (2007) and Li et al. (2011). In Table 1, the autocorrelations that exceed the 1% level of statistical significance are highlighted. To evaluate the significance of the autocorrelation coefficients, the freedom was estimated following Bartlett (1935). The length of the highlighted column for a particular month can be regarded as a measure of SST memory starting from that month (Lau and Yang, 1996). It can be seen that the Niño-3 SST anomalies originated from early summer can persist to winter. However, starting in spring and the previous winter, the significant autocorrelation of the Niño-3 index cannot easily move over spring, which implies a spring barrier of ENSO prediction (Webster and Yang, 1992).

It is interesting that early summer, when SST anomalies in the tropical central-eastern Pacific have their earliest potential prediction for SC winter rainfall, is the beginning season of ENSO development. Numerical studies have demonstrated that a credible skill level of ENSO prediction is at most six months ahead by multi-model ensemble (MME) forecasts (Jin et al., 2008). Therefore, the predictability of SC winter rainfall may still depend on the skill of ENSO prediction.

5. Decadal variability of the ENSO-SC rainfall relationship

Our statistical analyses demonstrate that the relationship between ENSO and SC winter rainfall shows a dominant covariant mode, and the two elements of the relationship are linked by anomalous anticyclones in the northwestern Pacific. In the past six decades, however, global surface temperature has been increasing and Pacific climate experienced a decadal regime shift in 1976/77. Under such a scenario, it is interesting to question whether the ENSO-SC winter rainfall relationship displays decadal variability over a long timescale.

To answer this, we performed 11-year running correlations for Niño-3 and SC rainfall indices, temporal coefficients of the leading SVD modes between global SST and rainfall over China, and PCs of the leading EOF mode of global SST and rainfall over China in boreal winter, respectively (Fig. 9). In all three time series, the correlations appear to be consistently significant before the early 1970s and after the early 1990s, but weaker between these times. Obviously, the three time series were obtained by three different methods, but all the correlations show similar decadal variability, which indicates that the decadal change of the ENSO-SC winter rainfall mode relationship is robust. Accordingly, we divided the six decades into three 20-year winters (1951/52–1970/71, 1971/72–1990/91 and 1991/92–2010/11) to examine the spatial differences of the ENSO-SC winter rainfall mode, respectively.

From 1951/52 to 1970/71, ENSO and SC winter rainfall indices are correlated at 0.47, exceeding the 95% confidence level. The spatial correlation of global SST and the SC winter rainfall index is similar to the central-Pacific El Niño-like pattern, with a significant positive correlation in the Niño-3.4 region and extending northeastward to the Californian coast, and a negative correlation surrounding the Pacific warm pool region (Fig. 10a). In addition, SSTs in the SCS and ESC

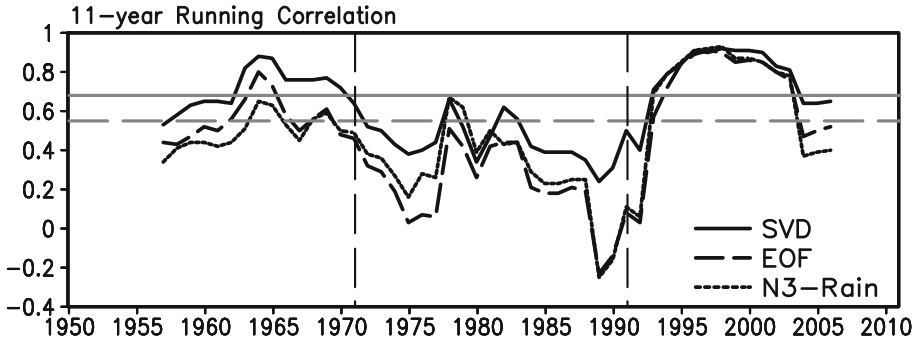

Fig. 9. 11-year running correlations of the winter rainfall over SC and Niño-3 indices (solid line), PCs of the leading EOF modes of global SST and rainfall over China in boreal winter (short-dashed line) and temporal coefficients of the leading SVD modes (long-dashed line).

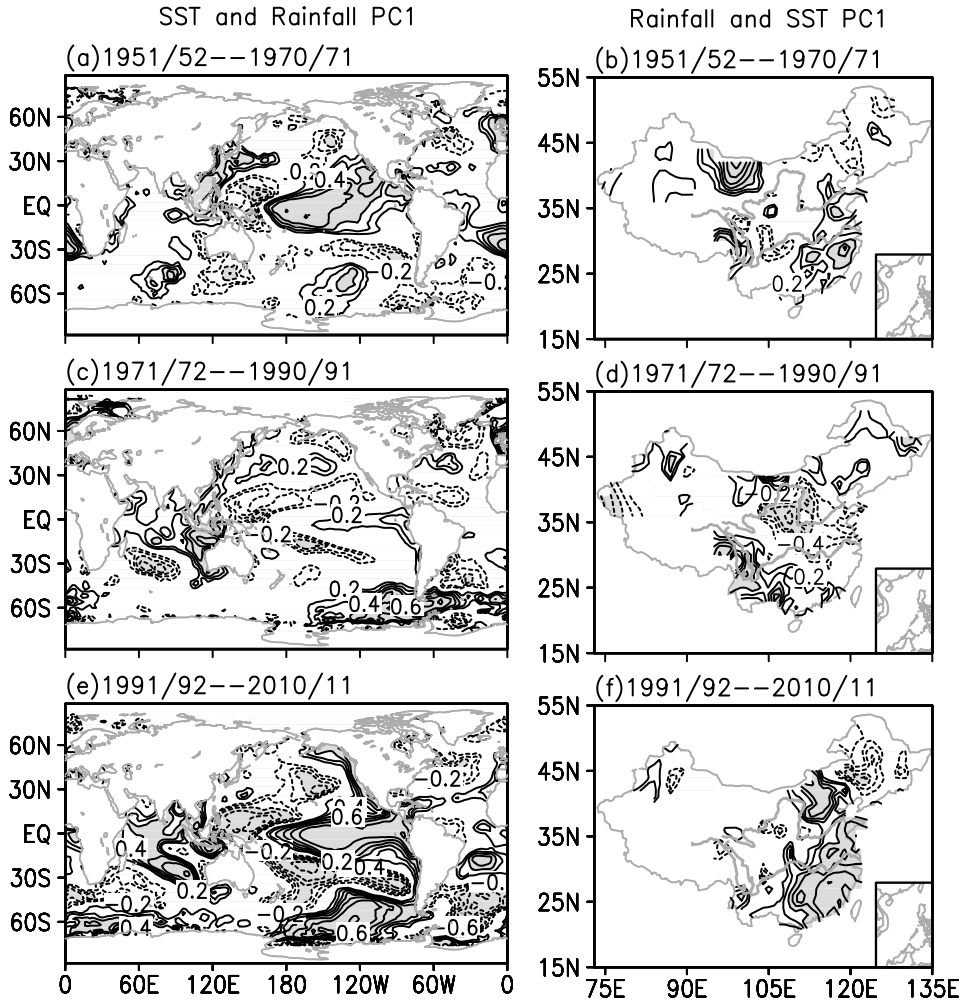

Fig. 10. Left panels: correlation of global SST with PC1 of rainfall over China. Right panels: correlation of rainfall over China with PC1 of global SST. (a) and (b): from 1951/52 to 1970/71; (c) and (d): from 1971/72 to 1990/91; (e) and (f): from 1991/92 to 2010/11. Contour intervals at 0.1, 0 and ±0.1 contours are omitted. Shadings represent regions with correlation coefficients more (less) than 0.4 (−0.4).

Table 1. Autocorrelations of the Niño-3 SST index for 1951–2010 as functions of the 12 calendar months with lagged time of 1–12 months. Autocorrelation coefficients significant at the 99% level are denoted by bold font.

	Jan	Feb	Mar	Apr	May	Jun	Jul	Aug	Sep	Oct	Nov	Dec
Feb	**0.93**											
Mar	**0.84**	**0.90**										
Apr	**0.56**	**0.70**	**0.81**									
May	0.37	**0.50**	**0.68**	**0.85**								
Jun	0.13	0.24	0.40	**0.61**	**0.87**							
Jul	−0.03	0.08	0.23	**0.49**	**0.70**	**0.88**						
Aug	−0.05	0.06	0.22	**0.49**	**0.68**	**0.84**	**0.96**					
Sep	−0.04	0.01	0.22	0.45	**0.66**	**0.81**	**0.88**	**0.91**				
Oct	−0.10	−0.05	0.12	0.36	**0.62**	**0.80**	**0.87**	**0.89**	**0.95**			
Nov	−0.10	−0.06	0.10	0.34	**0.61**	**0.78**	**0.84**	**0.87**	**0.92**	**0.98**		
Dec	−0.12	−0.08	0.08	0.32	**0.60**	**0.80**	**0.83**	**0.86**	**0.89**	**0.96**	**0.98**	
Jan	−0.16	−0.12	0.03	0.28	**0.53**	**0.74**	**0.78**	**0.81**	**0.86**	**0.94**	**0.95**	**0.96**
Feb		−0.10	0.03	0.23	0.45	**0.64**	**0.72**	**0.75**	**0.77**	**0.86**	**0.85**	**0.88**
Mar			0.01	0.21	0.45	**0.58**	**0.66**	**0.66**	**0.70**	**0.77**	**0.77**	**0.78**
Apr				−0.02	0.22	0.27	0.34	0.35	0.36	0.45	0.44	0.47
May					0.03	0.07	0.11	0.09	0.15	0.24	0.23	0.26
Jun						−0.17	−0.16	−0.17	−0.09	−0.01	0.01	0.03
Jul							−0.22	−0.24	−0.20	−0.12	−0.10	−0.12
Aug								−0.24	−0.21	−0.13	−0.12	−0.14
Sep									−0.14	−0.09	−0.08	−0.11
Oct										−0.14	−0.13	−0.15
Nov											−0.14	−0.16
Dec												−0.17

are also correlated significantly to SC winter rainfall. Meanwhile, the significant correlation of winter rainfall over China and the Niño-3 index resides mainly in the SC region and the western part of Inner Mongolia (Fig. 10b). During this period, in the warm phase of the ENSO cycle, a strong anomalous high reduces the East Asian trough and decreases meridional transport of cold air (Fig. 11a), thus weakening the East Asian winter monsoon (Fig. 12a). The anomalous anticyclone wind over the Philippines transports moisture toward the SC area (Fig. 12a) and then increases rainfall there (Fig. 10b), accompanied by a weak anomalous trough extending from western Inner Mongolia southward to the Indo-China peninsula (Fig. 11a).

From 1971/72 to 1990/91, the ENSO and SC winter rainfall indices are weakly related at 0.12, which is also supported by spatial correlation of global SST and the SC winter rainfall index (Fig. 10c). During this period, ENSO can significantly decrease rainfall over the vicinity of the Yellow River loop valley (YRLV) and increase rainfall over southwestern China, with no significant correlation in SC (Fig. 10d). In these 20 years, during the warm phase of the ENSO cycle, the East Asian trough deepens in the north and weakens in the south, and thus an anomalous trough extends from Northeast and North China to the southwest (Fig. 11b). Due to the weak anomalous anticyclone, the East Asian monsoon has not been obviously weakened (Fig. 12b). The YRLV is located near the anomalous trough and therefore winter rainfall is decreased there (Fig. 10d).

From 1991/92 to 2010/11, the ENSO and SC winter rainfall indices are highly correlated at 0.76, exceeding the 99.9% confidence level. The spatial correlation between global SST and the SC winter rainfall index exhibits a typical eastern-Pacific El Niño-like pattern, with a significant positive correlation in the Niño-3 region and a negative correlation surrounding the Pacific warm pool (Fig. 10e). During this period, it is interesting that IOB SST appears to correlate significantly with SC winter rainfall, while there seems to be no significant correlation in the SCS and ESC. Moreover, a significant positive correlation appears from the SC region extending northward to North China, and a negative correlation over Northeast China between winter rainfall over China and the Niño-3 index (Fig. 10f). In the most recent 20 years, in the warm phase of the ENSO cycle, an anomalous high stretches northwestward and weakens the East Asian trough, with a weak anomalous low laying in the south (Fig. 11c). Meanwhile, more moisture is transported by the anomalous anticyclone toward the SC region (Fig. 12c), converging over the SC and then increasing SC winter rainfall.

This analysis indicates that the relationship between ENSO and SC winter rainfall has undergone

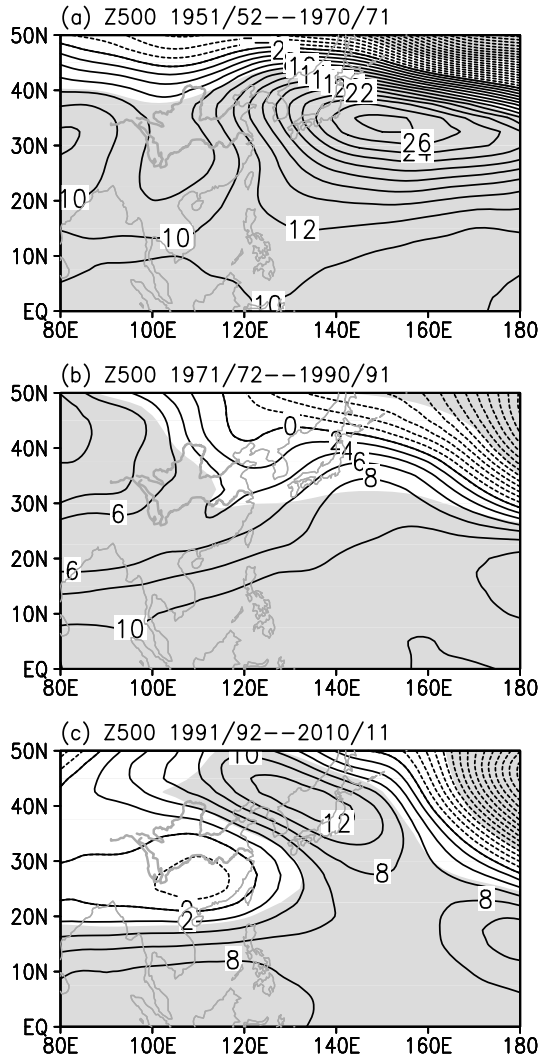

Fig. 11. Regression of geopotential height at 500 hPa on PC1 of global SST for (a) 1951/52–1970/71; (b) 1971/72–1990/91; and (c) 1991/92–2010/11. Shadings denote regions with correlation significant at the 95% confidence level.

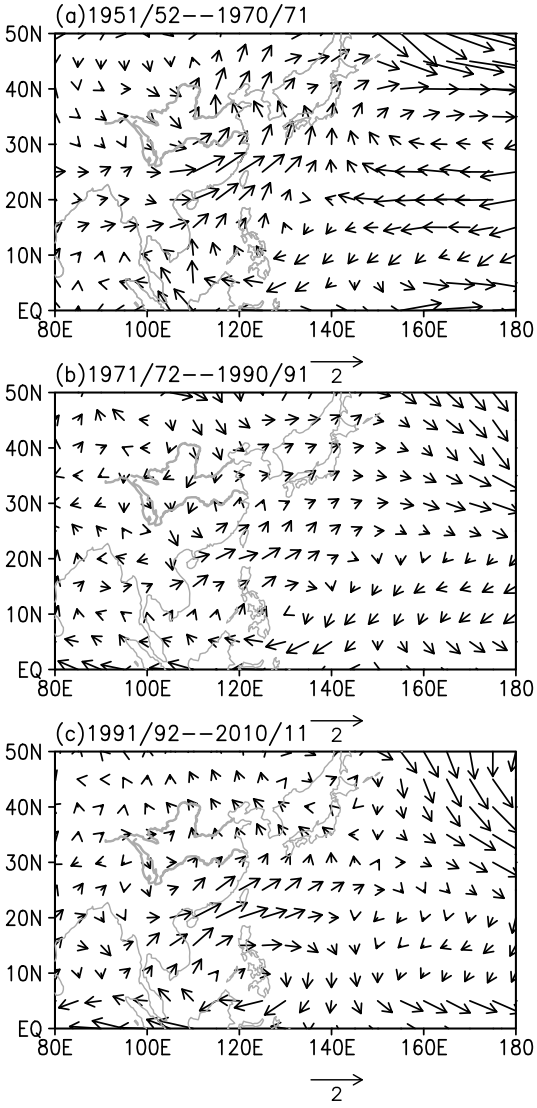

Fig. 12. Regression of horizontal wind at 850 hPa on PC1 of global SST for (a) 1951/52–1970/71; (b) 1971/72–1990/91; and (c) 1991/92–2010/11.

three different stages during the past six decades, with different atmospheric patterns and teleconnective processes in each stage. During every stage, the predictability of SC winter rainfall based on ENSO also shows dramatic differences (Fig. 13). For the first 20 years, SC winter rainfall has a potential predictability of half a year ahead, but the credibility of the prediction is low, reaching only the 90% confidence level. For the middle 20 years, SC winter rainfall seems unable to be predicted by ENSO. For the most recent 20 years, however, SC winter rainfall may not only be predicted by ENSO about half a year ahead, but also the credibility of the prediction is significantly enhanced, exceeding the 99% confidence level. In summary, the relationship between ENSO and SC winter rainfall is a close one during the first and last 20 years, but weak in the middle 20 years.

6. Summary and discussion

Based on station observations and reanalysis data, the relationship between ENSO and SC winter rainfall and its decadal variability were investigated with statistical analyses. The results show that ENSO can significantly influence SC winter rainfall via anomalous anticyclones in the northwestern Pacific. Winter rainfall over the SC region appears more (less) in El Niño (La Niña) years and has a potential predictability of about half a year ahead based on the ENSO cycle.

Furthermore, the relationship between ENSO and

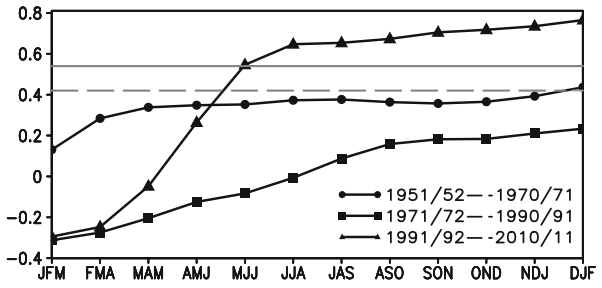

Fig. 13. As in Fig. 8, but for every two decades.

SC winter rainfall displays decadal variability, significant before the early 1970s and after the early 1990s, but much weaker between these times. For every stage, the atmospheric teleconnection seems quite different, and the potential predictability of SC winter rainfall also has large distinctions. In the most recent 20 years, the relationship between ENSO and SC winter rainfall is the most intimate, and the prediction of SC winter rainfall has its highest credibility.

The decadal variability of the relationship between ENSO and SC winter rainfall may be caused by the decadal variability of Walker circulation (Zeng et al., 2011), ENSO itself, external forcing [such as the Pacific Decadal Oscillation (PDO) and Atlantic Multidecadal Oscillation (AMO)], or changes of mean climate state due to global warming, which is out of the scope of this paper. Causes and mechanisms of the decadal modulation of the relationship between ENSO and SC winter rainfall remain unclear and need further examination. Further, this study suggests that it is necessary to consider decadal evolution of the relationship between predicted climate element and its predictor when we make climate prediction.

Acknowledgements. This study was supported by the National Natural Science Foundation of China (NSFC) (Grant Nos. 40906003 and 40830106) and the National Basic Research Program of China (Grant No. 2012CB 955603). Discussions with Drs. Jilin SUN and Xiaotong ZHENG were of great help.

REFERENCES

Alexander, M. A., I. Blade, M. Newman, J. R. Lanzante, N.-C. Lau, and J. D. Scotte, 2002: The atmospheric bridge: The influence of ENSO teleconnections on air-sea interaction over the global oceans. *J. Climate*, **15**, 2205–2231.

Bartlett, M. S., 1935: Some aspects of the time-correlation problem in regard to tests of significance. *Journal of the Royal Statistical Society* (*B*), **98**, 536–543.

Chen, J.-M., T. Li, and C.-F. Shih, 2007: Fall persistence barrier of sea surface temperature in the South China Sea associated with ENSO. *J. Climate*, **20**, 158–172.

Fu, C., and X. Teng, 1988: The relationship between ENSO and climate anomaly in China during the summer time. *Scientia Atmospherica Sinica*, Special Issue, 133–141. (in Chinese)

Huang, R.-H., and Y.-F. Wu, 1989: The influence of ENSO on the summer climate change in China and its mechanism. *Adv. Atmos. Sci.*, **6**, 21–31.

Jin, E. K., and Coauthors, 2008: Current status of ENSO prediction skill in coupled ocean-atmosphere models. *Climate Dyn.*, **31**, 647–664.

Ju, J., and J. M. Slingo, 1995: The Asian summer monsoon and ENSO. *Quart. J. Roy. Meteor. Soc.*, **121**, 1133–1168.

Kalnay, E., and Coauthors, 1996: The NCEP/NCAR 40-year reanalysis project. *Bull. Amer. Meteor. Soc.*, **77**, 437–471.

Kaplan, A., M. Cane, Y. Kushnir, A. Clement, M. Blumenthal, and B. Rajagopalan, 1998: Analyses of global sea surface temperature 1856–1991. *J. Geophys. Res.*, **103**, 18567–18589.

Lau, K.-M., and S. Yang, 1996: The Asian monsoon and predictability of the tropical ocean-atmosphere system. *Quart. J. Roy. Meteor. Soc.*, **122**, 945–957.

Lau, K.-M., and H. Weng, 2001: Coherent modes of global SST and summer rainfall over China: An assessment of the regional impacts of the 1997–98 El Niño. *J. Climate*, **14**, 1294–1308.

Li, C., and H. Ma, 2011: Coupled modes of precipitation over China and the Pacific sea surface temperature in boreal summertime. *Adv. Atmos. Sci.,* **28**, 1201–1214, doi: 10.1007/s00376-011-0127-3.

Li, C., L. Wu, and P. Chang, 2011: A far-reaching footprint of the tropical Pacific meridional mode on the summer rainfall over the Yellow River loop valley. *J. Climate.*, **24**, 2585–2598.

Rayner, N. A., and Coauthors, 2003: Global analyses of sea surface temperature, sea ice, and night marine air temperature since the late nineteenth century. *J. Geophys. Res.*, **108**, 4407, doi: 10.1029/2002JD002670.

Smith, T. M., and R. W. Reynolds, 2003: Extended reconstruction of global sea surface temperatures based on COADS data (1854–1997). *J. Climate*, **16**, 1495–1510.

Tao, S., and Q. Zhang, 1998: Response of the East Asian summer monsoon to ENSO events. *Scientia Atmospherica Sinica*, **22**, 399–407. (in Chinese)

Wang, B., R. Wu, and X. Fu, 2000: Pacific-East Asian teleconnection: How does ENSO affect East Asian Climate? *J. Climate*, **13**, 1517–1536.

Webster, P. J., and S. Yang, 1992: Monsoon and ENSO: Selectively interactive systems. *Quart J. Roy. Meteor. Soc.*, **118**, 825–877.

Webster, P. J., V. O. Magana, T. N. Palmer, T. A. Tomas, M. Yanai, and T. Yasunari, 1998: Monsoons: Processes, predictability, and prospects for prediction. *J. Geophys. Res.*, **103**, 14451–14510.

Wu, R., Z. Z. Hu, and B. P. Kirtman, 2003: Evolution of ENSO-related rainfall anomalies in East Asia. *J. Climate*, **16**, 3742–3758.

Xie, S.-P., and S. G. H. Philander, 1994: A coupled ocean-atmosphere model of relevance to the ITCZ in the eastern Pacific. *Tellus*, **46A**, 340–350.

Xie, S.-P., K. M. Hu, J. Hafner, H. Yokinaga, Y. Du, G. Huang, and T. Sampe, 2009: Indian Ocean capacitor effect on Indo-western Pacific climate during the summer following El Niño. *J. Climate.*, **22**, 730–747.

Xie, S.-P., Y. Du, G. Huang, X.-T. Zheng, H. Tokinaga, K. Hu, and Q. Liu, 2010: Decadal shift in El Niño influences on Indo-western Pacific and East Asian climate in the 1970s. *J. Climate*, **23**, 3352–3368.

Yang, J., Q. Liu, S.-P. Xie, Z. Liu, and L. Wu, 2007: Impact of the Indian Ocean SST basin mode on the Asian summer monsoon. *Geophys. Res. Lett.*, **34**, L02708, doi: 10.1029/2006GL028571.

Zhang, R., A. Sumi, and M. Kimoto, 1996: Impact of El Niño on the East Asian monsoon: A diagnostic study of the 86/87 and 91/92 events. *J. Meteor. Soc. Japan*, **74**, 49–62.

Zeng, G., W.-C. Wang, Z. B. Sun, and Z. X. Li, 2011: Atmospheric circulation cells associated with anomalous East Asian Winter Monsoon. *Adv. Atmos. Sci.*, **28**, 913–926, doi: 10.1007/s00376-010-0100-6.

Zhou, L. T., and R. Wu, 2010: Respective impacts of the East Asian winter monsoon and ENSO on winter rainfall in China. *J. Geophys. Res.*, **115**, D0217, doi: 10.1029/2009JD012502.

Zhou, L. T., C. Y. Tam, W. Zhou, and J. C. L. Chan, 2010: Influence of South China Sea SST and ENSO on winter rainfall over South China. *Adv. Atmos. Sci.*, **27**, 832–844, doi: 10.1007/s00376-009-9102-7.